UAV Photogrammetry Application to the Monitoring of Rubble Mound Breakwaters

Higinio González-Jorge, Ph.D.[1]; Iván Puente[2]; David Roca[3]; Joaquín Martínez-Sánchez, Ph.D.[4]; Borja Conde[5]; and Pedro Arias, Ph.D.[6]

Abstract: Monitoring of breakwaters is a key aspect to prevent failures that affect the safety and quality of service. Unmanned aerial vehicle (UAV) photogrammetry gives low-cost and accurate geometric data, flexibility, and productivity to perform aerial surveys, although the weather conditions restrict flights for wind speeds above 50 km/h (the Mikrokopter system). Despite the promising potential of these systems, its ability to monitor movement of cubes in breakwaters has not yet proven. The UAV photogrammetry is tested for the research reported in this paper in the Baiona breakwaters (northwestern Spain). A SD of 0.026 m is obtained from the point cloud. The detection limit of the system is evaluated and rotations lower than 1° could be detected. This value is calculated from the measurable differences in height values after the virtual rotation of a single cube. The system provides the exact position where the movement of the cube is produced and can be easily integrated with geographic information system–based management systems. **DOI: 10.1061/(ASCE)CF.1943-5509.0000702.**

Author keywords: Unmanned aerial vehicle (UAV); Photogrammetry; Breakwaters; Surveying; Monitoring.

Introduction

Ports are key infrastructures that serve as main hubs for channeling global trade. A port establishes a link between maritime and road/rail transportation, and allows freight shipping in a safe environment, protecting them from the marine environment (Segrelles 2000).

Traditionally, ports were built sheltered by coastal morphology. However, in recent years many outer ports were constructed due to the need of deeper seabed for larger vessels (Molinero-Guillén 2010; Corredor et al. 2013). These types of ports typically suffer severe attacks from waves that cause deterioration in the breakwater armoring, especially if maintenance is not properly performed. As it occurs with road pavements, gradual deterioration can often pass unnoticed until weak parts induce major damage. The earliest evidences of deterioration include displacement, breakage, or loss of armor units that must be properly monitored to perform a correct maintenance management. The periodic monitoring of a breakwater also provides damage data which can be linked to the prevailing sea conditions during the monitoring period for increasing the understating of failure mechanisms, and improving design and maintenance techniques (Gómez-Martín and Medina 2006; Lomónaco et al. 2009; Burcharth et al. 2010; Van Gent and Van der Werf 2010).

Most of the methods used for the monitoring of breakwaters are based on geomatic [i.e., total station measurements, aerial photogrammetry, aerial light detection and ranging (LiDAR), and terrestrial LiDAR] and hydrographic techniques (i.e., multibeam echo-sounders and sidescan sonar). Typically, geomatic techniques are used to measure the emerged area of the breakwaters and hydrographic techniques for the submerged parts (Kluger 1982; Mitchell et al. 2011; Molinés et al. 2012). The combined use of both methodologies provides a complete monitoring of the infrastructure (emerged and submerged parts).

Despite the amount of geomatic techniques to monitor the emerged area of the breakwaters, they have some weaknesses that make it interesting to investigate other possibilities.

Total stations are accurate instruments (<2 mm), although their productivity is very low when many points must be measured since the human operator must waste time targeting for each measurement. A rubble mound breakwater (distances of several kilometers are common) includes many units to be surveyed and a detailed control of all the units will waste many working days.

Terrestrial LiDAR typically shows lower accuracy than total stations. However, this accuracy is enough for the monitoring of breakwaters since the displacement of the units is typically larger than several centimeters and its accuracy is lower than 6 mm (Gonzalez-Jorge et al. 2011). Its main advantage is the high spatial resolution of the system that provides a dense three-dimensional (3D) point cloud of the structure. Productivity is higher than that achieved by a total station since the data acquisition is done automatically without targeting by a human operator. However,

[1]Dept. of Natural Resources and Environmental Engineering, School of Mining Engineering, Univ. of Vigo, Maxwell s/n, 36310 Vigo, Spain (corresponding author). E-mail: higiniog@uvigo.es

[2]Dept. of Natural Resources and Environmental Engineering, School of Mining Engineering, Univ. of Vigo, Maxwell s/n, 36310 Vigo, Spain. E-mail: ipuente@uvigo.es

[3]Dept. of Natural Resources and Environmental Engineering, School of Mining Engineering, Univ. of Vigo, Maxwell s/n, 36310 Vigo, Spain. E-mail: davidroca@uvigo.es

[4]Dept. of Natural Resources and Environmental Engineering, School of Mining Engineering, Univ. of Vigo, Maxwell s/n, 36310 Vigo, Spain. E-mail: joaquin.martinez@uvigo.es

[5]Dept. of Materials Engineering, Applied Mechanics and Construction, School of Industrial Engineering, Univ. of Vigo, Torrecedeira 86, 36208 Vigo, Spain. E-mail: bconde@uvigo.es

[6]Dept. of Natural Resources and Environmental Engineering, School of Mining Engineering, Univ. of Vigo, Maxwell s/n, 36310 Vigo, Spain. E-mail: parias@uvigo.es

Note. This manuscript was submitted on July 18, 2014; approved on October 13, 2014; published online on November 18, 2014. Discussion period open until April 18, 2015; separate discussions must be submitted for individual papers. This paper is part of the ***Journal of Performance of Constructed Facilities***, © ASCE, ISSN 0887-3828/04014194(8)/$25.00.

the requirement to use different base stations during the survey is also a limiting factor due the relative low measurement range (150–200 m in comparison with ranges over 1 km for total stations). Other problem is related to the sensor point of view that generates many occlusions in the point cloud and does not provide the complete geometric data of the structure (this problem is shared with total stations). These occlusions come from the shadows that some cubes produce on those that are behind. Aerial point of view is always more efficient to avoid this problem than terrestrial point of view. In addition, these systems exhibit high price and high computational cost in data processing due to the millions of points to be managed (González-Jorge et al. 2011). Point clouds larger than 10 million data are common. The automatic data acquisition provides points from many areas of no particular interest than must be then filtered by the human operator.

Aerial and mobile LiDAR shows higher productivity than terrestrial LiDAR due to the fact they are mounted on mobile platforms (planes, helicopters, vans, or vessels). Accuracy depends not only on the quality of the laser but also on the global navigation satellite system (GNSS) solution. The GNNS solution in real time kinematics (RTK) mode provides accuracies around 2 cm in xy and 4 cm in z for high-performance systems, while LiDAR sensor give accuracies similar to those obtained with terrestrial systems (6 mm). Combined accuracy is poorer than that obtained from a terrestrial LiDAR system but enough for monitoring centmetric displacements of cubes in breakwaters. They do not present many occlusions because of its overhead point of view, especially those mounted on aerial systems. One of the main problems is the high cost of aerial and mobile LiDAR systems, and the cost of the plane or helicopter flights. Computation cost is also high because they provide point clouds even larger than those obtained from terrestrial LiDAR; 100 million points are common (Pirotti et al. 2013; Puente et al. 2013; Reif et al. 2013).

Aerial photogrammetry depicts some of the restrictions of aerial LiDAR due to the high cost of photogrammetric flights and photogrammetric cameras. Accuracy is lower than that in aerial LiDAR (between 5 and 10 cm is common); however, many ports in the world still use this systems to detect movements in breakwaters (Wiechert et al. 2010; Merchant 2012).

Unmanned aerial vehicles (UAVs) reach today high levels of development that allow its use in a robust and simple form, presenting very affordable prices, even for professional systems. Operators must take care with weather conditions, especially with wind speed in coastal areas. Flights are typically limit to speeds lower than 50 km/h. Low-cost UAVs allow professional features as waypoints navigation, battery autonomies near to 30 min, and the possibility of carrying payloads of around 2–3 kg. This payload allows including systems as digital cameras to perform aerial photogrammetry. Flight heights are smaller (30–50 m) than those from manned systems. As a result, simpler photographic equipment used in UAV systems can achieve the same precision of the traditional manned aerial photogrammetry. Unmanned aerial vehicles' photogrammetry has shown reliable applications for the inspection of large structures (http://www.aibotix.com), generation of digital terrain models, environmental studies, or cultural heritage inventory (Colomina et al. 2014; Nex et al. 2014).

The bibliography does not show applications of UAV photogrammetry to the monitoring of rubble mound breakwaters. Therefore, this paper presents an UAV photogrammetry procedure to monitor displacements in rubble mound breakwaters and the detection limit of the described procedure to prove the real possibilities of the methodology in this field of application.

Materials and Methods

Area of Study

The rubble mound breakwater used for the research reported in this paper is the one that protects the Port of Baiona, placed in northwestern Spain, on the Atlantic coast of Galicia (42.124792° N; −8.844616°E). Baiona is famous because on March 1, 1493, La Pinta ship arrived to its port in the return trip from the discovery of America (Christopher Columbus expedition). Nowadays Baiona is a touristic village and its port is mainly used for yachting. Baiona breakwaters (Fig. 1) are made of single-layer cubes of 1.2 m, whose main characteristics are 340-m long, a crest width and height of 8.4 and 8.5 m (respectively), and a structure base width of 21.7 m with a 49° slope angle. Baiona village suffers severe Atlantic storms during winter, causing significant deterioration in its civilian infrastructures, including the port. It is therefore important to develop monitoring procedures to improve the infrastructure management.

Data Acquisition

The UAV system used for the research reported in this paper is a Mikrokopter Okto XL (http://www.mikrokopter.de; Fig. 2). It is a medium-cost UAV powered by eight brushless motors that includes carbon fiber/aluminum fuselage. The UAV includes a flight control with a global positioning system (GPS) positioning, three-axis accelerometer, three-axis gyroscope, magnetometer, and pressure sensor. A Sony Nex 7 camera (http://www.sony.com/uk) has been mounted on the aerial unit. This captures red-green-blue (RGB) images with 24.3-megapixel (Mpx) resolution. Mounted lens is a Sony SEL16F28 with a focal length of 16 mm (F2.8).

Data acquisition was first planned in the laboratory using georeferenced images and the planning software of the Mikrokopter system. The software generates GPS waypoints for the survey that are uploaded to the flight control of the Mikrokopter Okto XL. The breakwaters, UAV height (25 m), and the distance between waypoints were chosen in a way that images overlap approximately 75%.

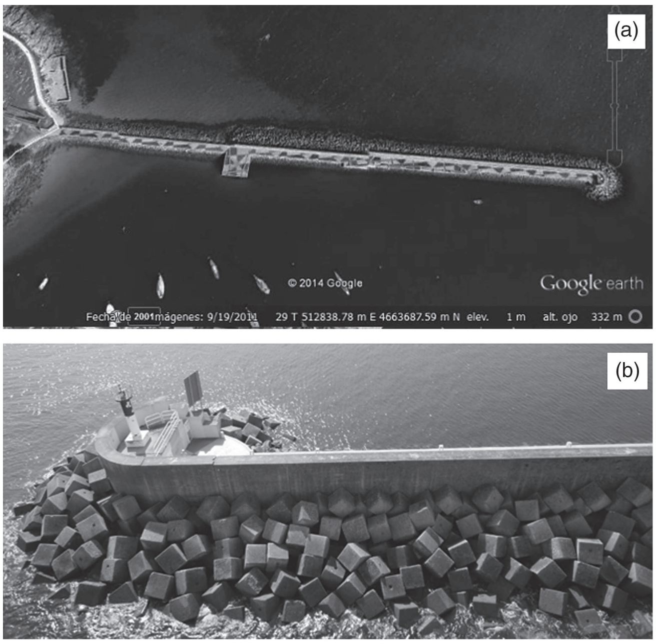

Fig. 1. (a) Baiona port and breakwaters, highlighted (© 2014 Google); (b) breakwaters detail (image by David Roca)

Fig. 2. Mikrokopter UAV with Sony Nex 7 during survey (image by Higinio González-Jorge)

This operation is essential for a proper post processing photogrammetric restitution. The human pilot is the responsible for the takeoff and landing operations. The surveying is done using the waypoints for an automatic navigation. A total of 68 images were acquired.

Ground references (28 points) are measured using a GPS Settop AL-102 to provide information for data registration. The GPS system was used in RTK mode with an accuracy of 2 cm in horizontal and 3.5 cm in vertical values.

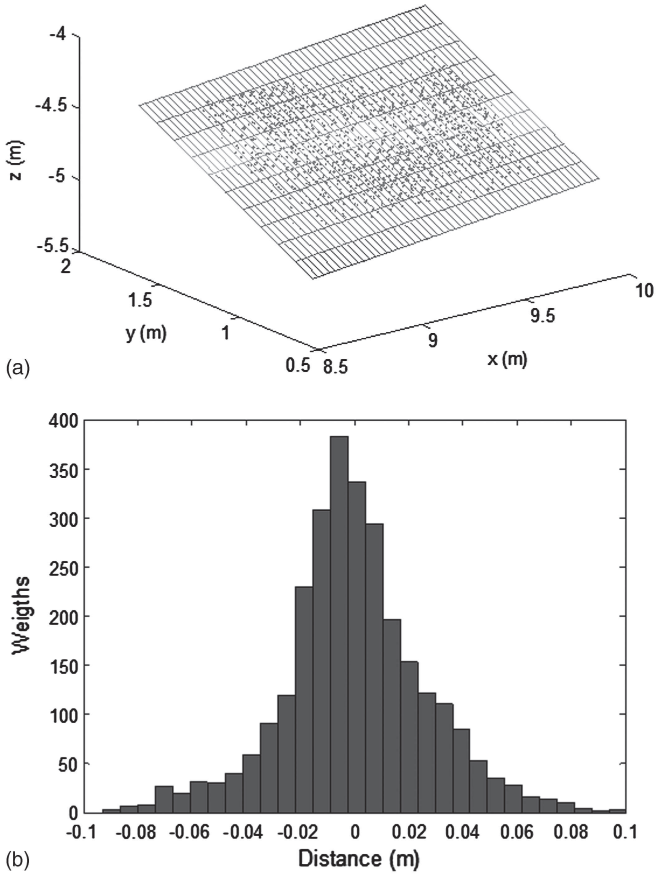

Fig. 4. (a) Plane fitting of the point cloud from a cube face; (b) distribution of distances between each individual point and the fitted surface

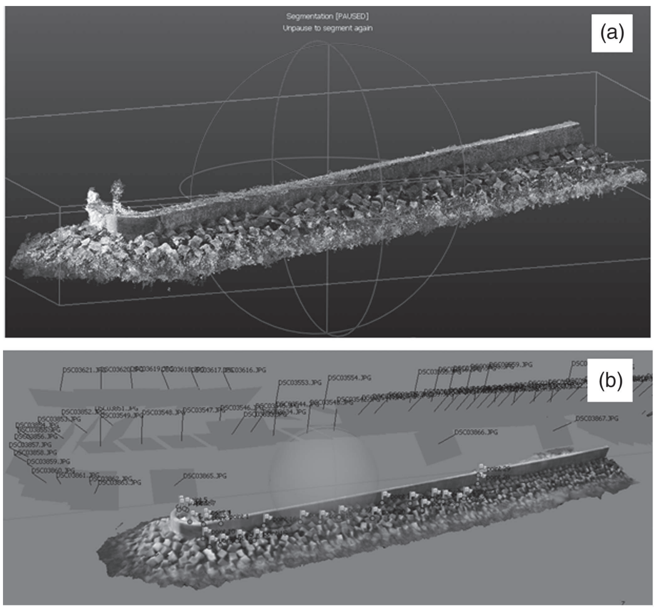

Fig. 3. Three-dimensional model after *Photogrammetry Workbench* processing: (a) point cloud; (b) surfaces model; images were exported from the *Photogrammetry Workbench* software

Data Processing

Photogrammetry Workbench from University of Salamanca (Spain) was used for image data processing (Atkinson 2001). The software uses computer vision algorithms for the automatic extraction of characteristic points of images. Because coastal

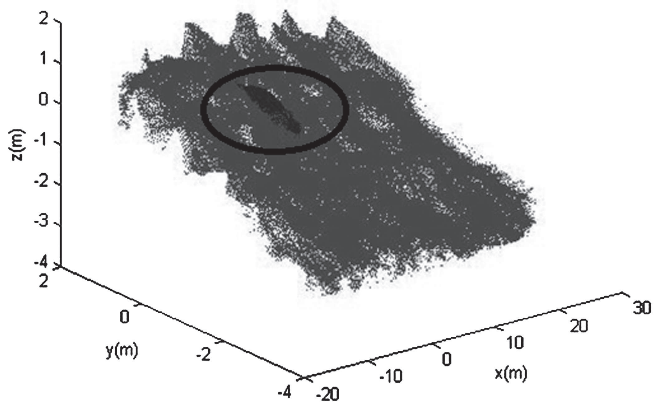

Fig. 5. Segmented unit (highlighted) and the rest of the armor units of the breakwaters

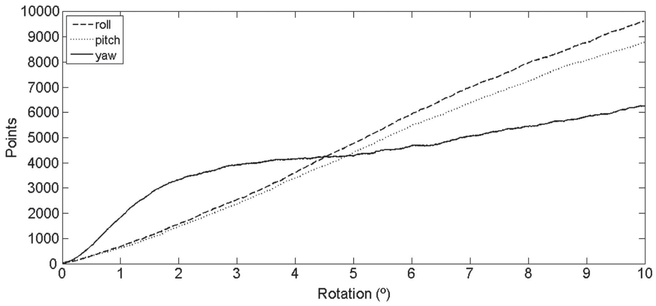

Fig. 6. Number of displaced points detected with roll, pitch, and yaw rotations between 0 and 10°

monitoring scenes usually present variations in scale and illumination, classical algorithms based on grey levels, such as area-based matching (ABM; Joglekar and Gedam 2012) and least-square matching (LSM; Gruen 1985), are useless. In this sense, the scale-invariant affine transform (ASIFT) algorithm has been incorporated into *Photogrammetry Workbench* (Morel and Yu 2009). The ASIFT includes the consideration of two additional parameters that control the presence of images with different scales and rotations.

The correspondence points derived from the ASIFT algorithm are the input for the orientation procedure, which is performed in two steps, as follows: (1) a pairwise orientation is executed by relating the images to each other by means of the Longuet-Higgins (1987) algorithm, and (2) this initial and relative

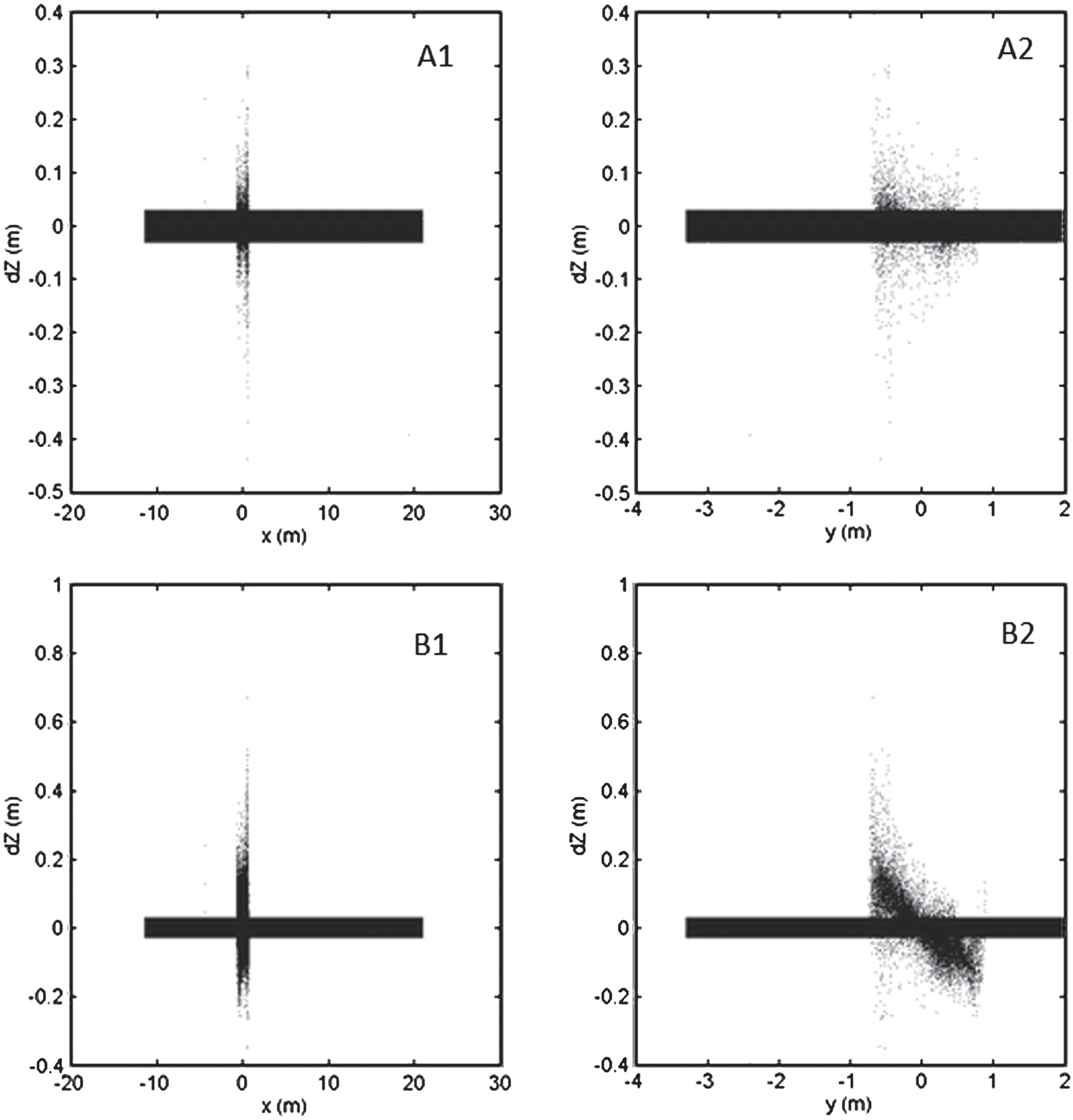

Fig. 7. Differences in z values of the point cloud under roll rotation: (a) 1°; (b) 10°

approximation to the solution is used to perform a global orientation adjustment between all images by means of collinearity equations (Kraus 1993) which could include the determination of the camera parameters (self-calibration).

The absolute orientation is completed with the 28 GPS points previously measured. At the end of this process a georeferenced point cloud of the breakwaters is obtained (Fig. 3).

Evaluation of the Detection Limit

The next step involves the evaluation of the detection limit using UAV, photogrammetry surveying of breakwaters. This test is essential to establish whether the accuracy provided by this technique is enough for monitoring small shifts in armor units.

The first step tests the precision of the UAV photogrammetry. One face of one cube of the armor is manually segmented using

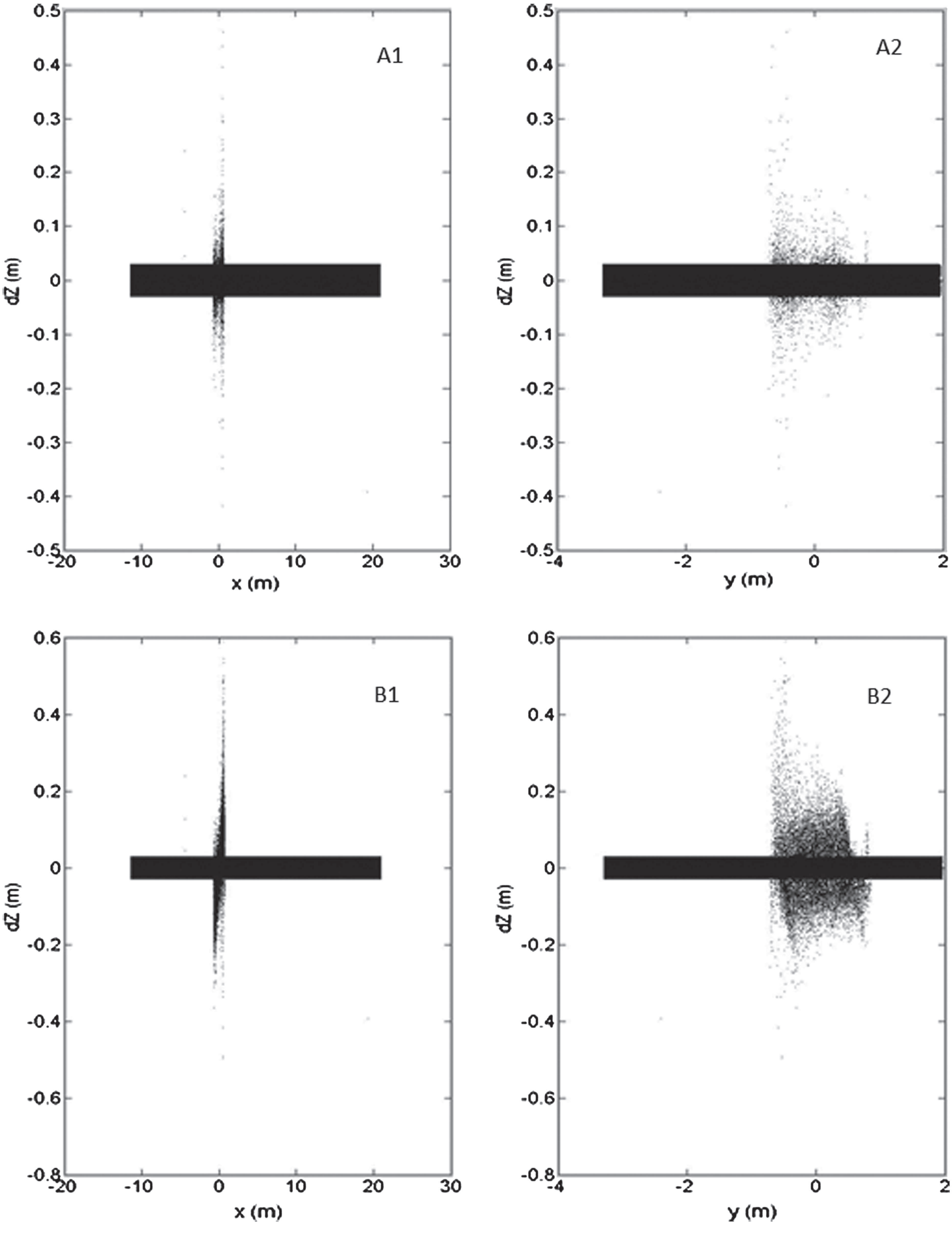

Fig. 8. Differences in z values of the point cloud under pitch rotation: (a) 1°; (b) 10°

cloud compare software. *Cloud Compare* is a 3D point cloud processing software including algorithms for registration, resampling, statistics computation, sensor management, interactive segmentation, and display enhancement.

A plane is fitted using a least-square algorithm implemented in *MatLAB* software (Fig. 4). The distance d_i of any point x_i, y_i from the least-square best-fit plane is given by

$$d_i = ax_i + by_i + cz_i \tag{1}$$

where the direction cosines of the normal to the plane are (a, b, c). The function used to minimization is therefore

$$E = \sum_{i=1}^{n} d_i^2 = \sum_{i=1}^{n} (ax_i + by_i + cz_i)^2 \tag{2}$$

where E = sum of the squared distances; and n = number of points.

Distances d_i between the points and the fitted surface show a Gaussian distribution with a SD (σ) of 0.026 m ($2\sigma = 0.052$ m;

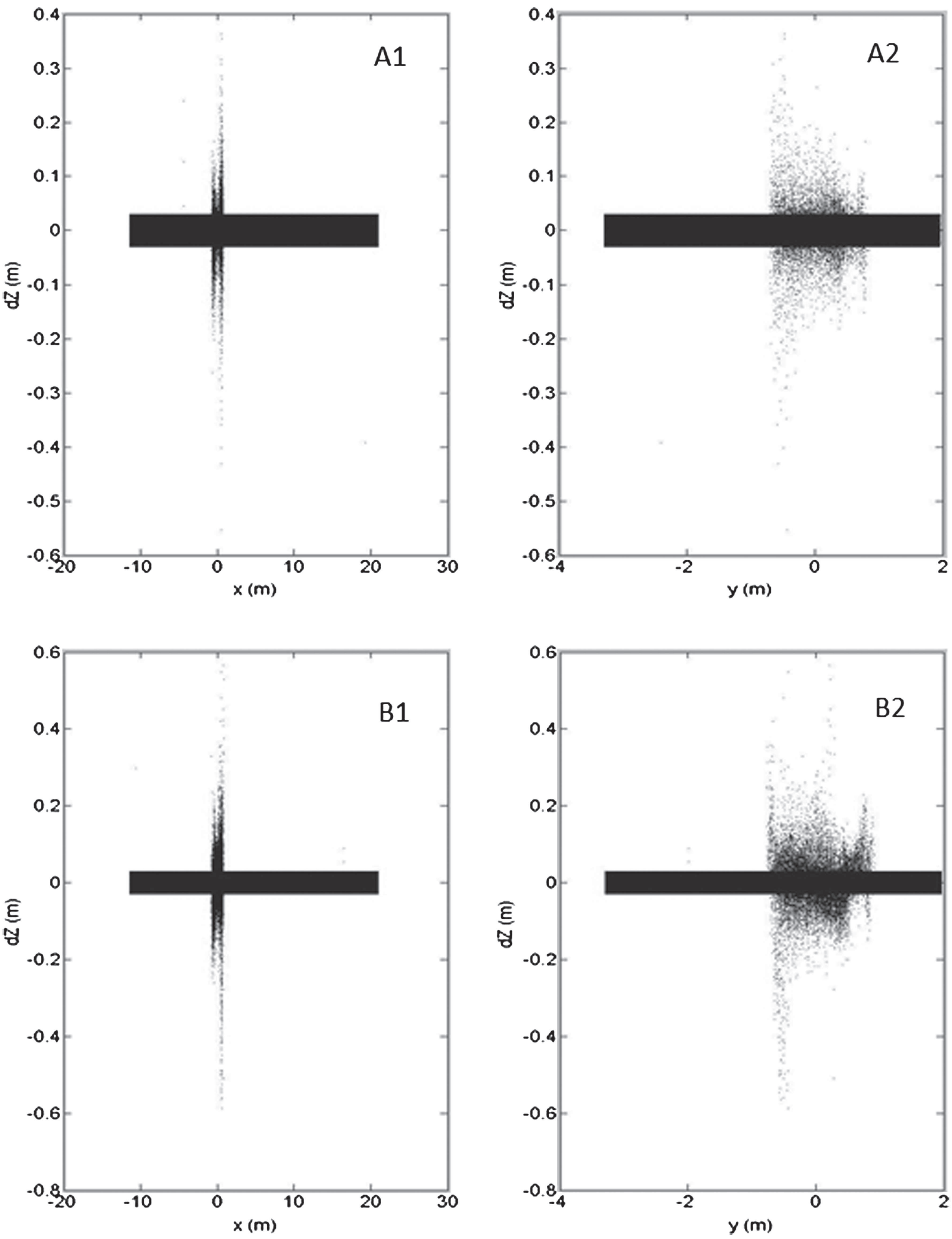

Fig. 9. Differences in z values of the point cloud under yaw rotation: (a) 1°; (b) 10°

95% coverage). According to this, any changing distance over 0.052 m between two inspection surveys could be indicative of an armor unit displacement with a probability of 95%. This value will be assumed as the threshold to provide an alert in monitoring of breakwaters system. Other errors like point cloud registration are not taken into account because they are typically lower than 0.005 m.

The subsequent step consists in the determination of the detection limit of the system (the minimum movement that can be distinguished). The movement of an armor unit can be decomposed in six main components; three translations and three rotations. However, due to the block to block interaction, the spatial rotation is the most probable movement. There is no flat foundation surface beneath the cubes so in this paper only rotational movements are evaluated.

Additional steps of the procedure include the following:

- Point cloud preparation for simulation. A single cube is manually segmented from the point cloud (Fig. 5). In this way, the movement of the cube is allowed by referring to the original point cloud using rotation matrices. These separated point clouds are later used as the inputs to the algorithm developed to check the sensitivity of the UAV photogrammetry method.
- Rotation of the previously segmented armor cube. A rotation center is established in the geometrical center of the cube. A rotation loop is programmed from 0 to 10° with a step of 0.02° (roll, pitch, and yaw angles). It is assumed that the sensitivity of the method will be better than 10°, so higher angles are not tested.
- Generation of Gaussian noise. Only data from one survey could be used for the evaluation of the detection limit since there are not more data available. The precision of the method was previously calculated (Fig. 4) with the plane fitting. This data is used to provide the Gaussian noise. Once one rotation step is done, Gaussian noise is applied to the whole point cloud according to the precision data, including the rotated armor cube. Thus, although only one point cloud is used, the lack of precision during different surveys is taken into account in the calculations.
- Displacement detection. Every point cloud of the breakwater unit generated after each step rotation (including Gaussian noise) is compared with the input survey data. For the comparison, the unorganized point clouds are converted into organized point clouds using a nearest neighbor algorithm. This algorithm, also known as proximal interpolation, approximates the value of a z data for a nongiven point in an xy organized network by the z value of the nearest xy data in the unorganized point cloud (Bolstad 2008). Hence, the differences between points can be computed as differences in the z data values. Differences over 0.052 m (2σ) could be measurable by the UAV photogrammetry technique. They are correlated with the roll, pitch, and yaw rotation of the cube.

Results and Discussion

Fig. 6 shows the number of points that can be detected for a certain rotation angle. These points represent differences against the original point cloud higher than 0.052 m. Even for small rotations of the cube (around 0.1°) some evidence of movement can be detected (around 100 points over the threshold). The number of points displaced increases with the angular rotation. For smaller angles (between 0 and 4°), evidences of yaw rotation are more important than evidences of roll and pitch rotation. This trend changes for angles higher than 5°, where roll and pitch show more displaced points.

Figs. 7–9 show the differences in z values for roll, pitch, and yaw rotations of the cube (angles 1 and 10°). The differences in z increase with the increasing of rotation angle in all directions. This is related to the greater number of points that are above the detection threshold (Fig. 6). A significant number of points still appear around $dz = 0 \pm 0.052$ m that correspond to those whose difference is within the system error. Graphs from Figs. 8–10 allow the precise location of the displaced cubes. This type of information could be of great help to improve the maintenance and management of breakwaters because it allows the damage location.

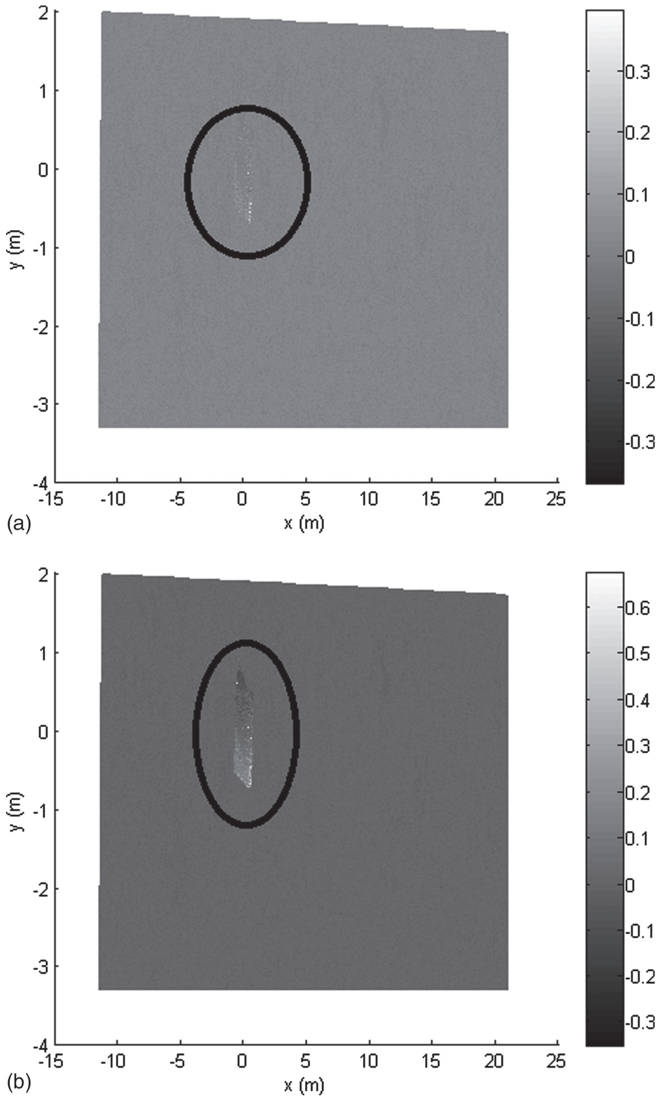

Fig. 10. Image of z changes for roll rotations of (a) 1°; (b) 10°; area where the block is rotated is highlighted; right grayscale shows the z displacement (codified in meters)

Fig. 10 shows a range image where the color bar indicates the differences in z values between the initial survey and the data generated after 1 and 10° roll rotations. This type of image appears very visual and easy to understand, also being easily incorporated into a GIS program.

Conclusions

An UAV low-cost photogrammetry technique is developed for monitoring rubble mound breakwaters. It appears as a productive and reliable technique if wind conditions keep below 50 km/h

(Mikrokopter system). The system is tested at the Baiona port in northwestern Spain.

The SD of the technique was evaluated on the flat face of one of the cubes with values of 0.026 m ($2\sigma = 0.052$ m; 95% coverage). The detection limit of the technique was measured creating artificial rotations in roll, pitch, and yaw for one specific cube. Gaussian noise was introduced in the simulation taking into account the SD of the survey to make the results more reliable, according to the precision data obtained from the survey.

Changes in the point cloud after rotations were monitored calculating the distances between both datasets. The detection of any difference in height is assumed that come from the rotation of the cube. The technique shows that rotations even lower than 1° could be detected. These angular differences produce dimensional changes in z higher than 10 cm. These changes could be easily monitored since there are over the SD of the measurements.

It is recommended to study in further works the influence of the accuracy of the UAV photogrammetry method with camera resolution, flight height, focal length, and the position of GPS controls points.

Acknowledgments

The writers want to give thanks to the Spanish Ministry of Economy and Competitiveness, and Xunta de Galicia for the financial support given; and Human Resources programs (BES-2010-034106 and IPP055—EXP44) and project (Grant No. EM2013/005).

References

Atkinson, K. B. (2001). *Close range photogrammetry and machine vision*, Whittles, Dunbeath, U.K.

Bolstad, P. (2008). *GIS fundamentals: A first text on geographic information systems*, Attlas, Ashland, OH.

Burcharth, H. F., Andersen, T. L., and Medina, J. R. (2010). “Stability of cubipod armoured roundheads in short-crested waves. A comparison between cubipod and cube armour stability.” *Coastal Eng.*, 32, 1–10.

Cloud Compare v2.5.4.1 [Computer software]. License GNU GPL.

Colomina, I., and Molina, P. (2014). “Unmanned aerial systems for photogrammetry remote sensing: A review.” *ISPRS J. Photogramm.*, 92, 79–97.

Corredor, A., Santos, M., Peña, E., Maciñeira, E., Gómez-Martín, M. E., and Medina, J. (2013). “Designing and constructing cubipod armored breakwaters in the ports of Malaga and Punta Langosteira (Spain).” *Proc., Institution of Civil Engineers (ICE) Coasts, Marine Structures and Breakwaters Conf.*, London.

Gómez-Martín, M. E., and Medina, J. R. (2006). “Damage progression on cube armored breakwaters.” *Proc., Int. Conf. on Coastal Engineering (ICCE)*, 5229–5240.

González-Jorge, H., Riveiro, B., Armesto, J., and Arias, P. (2011). “Standard artifact for the geometric verification of terrestrial laser scanning systems.” *Opt. Laser Technol.*, 43(7), 1249–1256.

Gruen, A. (1985). “Adaptive least squares correlation: A powerful image matching technique.” *South Afr. J. Photogramm. Remote Sens. Cartogr.*, 14(3), 175–187.

Joglekar, J., and Gedam, S. (2012). “Area based image matching methods—A survey.” *Int. J. Emerg. Technol. Adv. Eng.*, 2(5), 2250–2459.

Kluger, J. W. (1982). “The monitoring of rubble mound breakwater stability using a photographic survey method.” *Coastal Eng.*, 2164–2170.

Kraus, K. (1993). “Photogrammetry.” *Fundamentals and standard processes*, Dümmler, Bonn, Germany.

Lomónaco, P., Vidal, C., Medina, J. R., and Gómez-Martín, M. E. (2009). “Evolution of damage roudheads protected with cube and cubipod armour units.” *Proc., Institution of Civil Engineers (ICE) Coastal, Marine Structures and Breakwaters Conf.*, London, 169–180.

Longuet-Higgins, H. C. (1987). “A computer algorithm for reconstructing a scene from two projections.” *Readings in computer vision: Issues, problems, principles, and paradigms*, M. A. Fisher and O. Firschein, eds., Morgan Kaufmann Publishers, San Francisco, CA, 61–62.

MatLAB [Computer software]. Natick, MA, Mathworks.

Merchant, D. C. (2012). “Aerial camera metric calibration. History and status.” *Proc., American Society for Photogrammetry and Remote Sensing (ASPRS) Annual Conf.*, Bethesda, MD, 380–389.

Mitchell, T., and Chang, M. (2011). “Utilizing vessel based mobile LiDAR and bathymetry survey techniques for survey of four southern California breakwaters.” *Coastal Eng. Pract.*, 957–969.

Molinero-Guillén, P. (2010). “Construction of large port infrastructures at the north of Spain.” *Proc., del Congreso de Ingeniería Civil*, Madrid, Spain, 1–20.

Molinés, J., Piedad-Herea, M., Pérez, T., and Medina, J. R. (2012). “Laser scanner technique to quantify randomness in cube and cubipod armour layers.” *Coastlab Conf.*, P. Troch, V. Stratigaki, and S. De Roo, eds., Universiteit Gent, Ghent, Belgium.

Morel, J. M., and Yu, G. (2009). “ASIFT: A new framework for fully affine invariant image comparison.” *SIAM J. Imag. Sci.*, 2(2), 438–469.

Nex, F., and Remondino, F. (2014). “UAV for 3D mapping applications: A review.” *Appl. Geomatics*, 6(1), 1–15.

Photogrammetric Workbench 1.0 [Computer software]. Spain, Univ. of Salamanca.

Pirotti, F., Guarmeri, A., and Vettore, A. (2013). “State of the art of ground and aerial laser scanning technoloqies for high-resolution topography of the earth surface.” *Eur. J. Remote Sens.*, 46(1), 66–78.

Puente, I., González-Jorge, H., Martínez-Sánchez, J., and Arias, P. (2013). “Review of mobile mapping and surveying technologies.” *Measurement*, 46(7), 2127–2145.

Reif, M. K., Wozencraft, J. M., Dunkin, L. M., Sylverter, C. S., and Macon, C. L. (2013). “A review of U.S. Army Corps of Engineers airborne coastal mapping in the Great Lakes.” *J. Remote Sens. Great Lakes Other Inland Waters*, 39(S1), 194–204.

Segrelles, J. A. (2000). “The ports, the global economy and planning.” *Geog. J. Uruguay*, 117–137.

Van Gent, M. R. A., and Van der Werf, I. M. (2010). “Stability of breakwater roundheads during construction.” *Coastal Eng.*, 32, 1–15.

Wiechert, A., and Gruber, M. (2010). “Ten years large format digital aerial cameras: A review.” *Proc., American Society for Photogrammetry and Remote Sensing (ASPRS) Annual Conf.*, Bethesda, MD, 217–221.